

1 **Choosing the right tool for the job: A comprehensive assessment of serological assays**  
2 **for SARS-CoV-2 as surrogates for authentic virus neutralization**

3  
4 Nicholas Wohlgemuth<sup>1</sup>, Kendall Whitt<sup>2</sup>, Sean Cherry<sup>1</sup>, Ericka Kirkpatrick Roubidoux<sup>1</sup>, Chun-  
5 Yang Lin<sup>3</sup>, Kim J. Allison<sup>1</sup>, Ashleigh Gowen<sup>1</sup>, Pamela Freiden<sup>1</sup>, E. Kaitlynn Allen<sup>3</sup>, St. Jude  
6 Investigative Team, Aditya H. Gaur<sup>1</sup>, Jeremie H. Estep<sup>4,5</sup>, Li Tang<sup>6</sup>, Tomi Mori<sup>6</sup>, Diego R.  
7 Hijano<sup>1</sup>, Hana Hakim<sup>1</sup>, Maureen A. McGargill<sup>3</sup>, Florian Krammer<sup>7</sup>, Michael A. Whitt<sup>2</sup>, Joshua  
8 Wolf<sup>1</sup>, Paul G. Thomas<sup>3</sup>, Stacey Schultz-Cherry<sup>1\*</sup>

9  
10 St. Jude Investigative Team

11 David C. Brice<sup>3</sup>, Ashley Castellaw<sup>3</sup>, David E. Whittman<sup>8</sup>, Jason Hodges<sup>4</sup>, Ronald H. Dallas<sup>1</sup>,  
12 Valerie Cortez<sup>1</sup>, Ana Vazquez-Pagan<sup>1</sup>, Richard J. Webby<sup>1</sup>, Resha Bajracharya<sup>3</sup>, Brandi L Clark<sup>3</sup>,  
13 Lee-Ann Van de Velde<sup>3</sup>, Walid Awad<sup>3</sup>, Taylor L Wilson<sup>3</sup>, Allison M. Kirk<sup>3</sup>, Elaine I. Tuomanen<sup>1</sup>,  
14 Randall T. Hayden<sup>9</sup>, James Hoffman<sup>10</sup>, Jamie Russell-Bell<sup>1</sup>, James Sparks<sup>5</sup>

15  
16 <sup>1</sup>Department of Infectious Diseases, St Jude Children's Research Hospital, Memphis, TN, USA

17 <sup>2</sup>Department of Microbiology, Immunology and Biochemistry, University of Tennessee Health  
18 Science Center, Memphis, TN, USA

19 <sup>3</sup>Department of Immunology, St Jude Children's Research Hospital, Memphis, TN, USA

20 <sup>4</sup>Department of Hematology, St Jude Children's Research Hospital, Memphis, TN, USA

21 <sup>5</sup>Department of Global Pediatric Medicine, St Jude Children's Research Hospital, Memphis, TN,  
22 USA

23 <sup>6</sup>Department of Biostatistics, St Jude Children's Research Hospital, Memphis, TN, USA

24 <sup>7</sup>Department of Microbiology, Icahn School of Medicine at Mount Sinai, New York, NY, USA

25 <sup>8</sup>Office of Quality and Patient Care St Jude Children's Research Hospital, Memphis, TN, USA

26 <sup>9</sup>Department of Pathology, St Jude Children's Research Hospital, Memphis, TN, USA

- 27 <sup>10</sup>Department of Pharmaceutical Sciences, St Jude Children's Research Hospital, Memphis, TN,  
28 USA  
29 \*Corresponding author: Stacey-Schulz-Cherry [stacey.schultz-cherry@stjude.org](mailto:stacey.schultz-cherry@stjude.org)

30 **Severe acute respiratory syndrome coronavirus 2 (SARS-CoV-2) emerged in late 2019**  
31 **and has since caused a global pandemic resulting in millions of cases and deaths<sup>1-4</sup>.**  
32 **Diagnostic tools and serological assays are critical for controlling the outbreak<sup>5-7</sup>,**  
33 **especially assays designed to quantitate neutralizing antibody levels, considered the**  
34 **best correlate of protection<sup>8-11</sup>. As vaccines become increasingly available<sup>12</sup>, it is**  
35 **important to identify reliable methods for measuring neutralizing antibody responses**  
36 **that correlate with authentic virus neutralization but can be performed outside of**  
37 **biosafety level 3 (BSL3) laboratories. While many neutralizing assays using pseudotyped**  
38 **virus have been developed, there have been few studies comparing the different assays**  
39 **to each other as surrogates for authentic virus neutralization<sup>9,10,13,14</sup>. Here we**  
40 **characterized three enzyme-linked immunosorbent assays (ELISAs) and three**  
41 **pseudotyped VSV virus neutralization assays and assessed their concordance with**  
42 **authentic virus neutralization. The most accurate assays for predicting authentic virus**  
43 **neutralization were luciferase and secreted embryonic alkaline phosphatase (SEAP)**  
44 **expressing pseudotyped virus neutralizations, followed by GFP expressing pseudotyped**  
45 **virus neutralization, and then the ELISAs.**

46 Numerous serological assays have been developed to quantitate severe acute  
47 respiratory syndrome coronavirus 2 (SARS-CoV-2) antibody responses to determine total  
48 antibody concentration and neutralization activity. Neutralization assays can be performed with  
49 authentic virus or a pseudotyped virus expressing the SARS-CoV-2 spike (S) protein on its  
50 surface and a marker to measure infection of cells. The clear advantage of a pseudotyped virus  
51 is safety, as these studies can be performed in standard BSL2 laboratories. Another advantage  
52 is that results using pseudotyped virus can be obtained sooner, typically less than 24 hours  
53 whereas with authentic virus, plaque reduction-based neutralization assays take 2-3 days. A  
54 third advantage of using pseudotypes is flexibility. Pseudotypes expressing spike variants can  
55 be generated easily once the sequence is known since all that is needed is a plasmid that

56 expresses the variant of interest. One disadvantage of the pseudotyped virus neutralization  
57 assay is the pseudotyped viruses lack all but the spike protein from SARS-CoV-2, meaning they  
58 can only be neutralized by spike specific antibodies, and the clustering of proteins may not be  
59 representative of authentic virus particles. Yet, few studies have demonstrated whether the  
60 neutralization dose 50% (ND<sub>50</sub>), the dilution at which 50% of virus will be neutralized, differs  
61 between pseudotyped virus detection platforms and, importantly, how they compare to authentic  
62 virus. To fill this gap in knowledge, we compared SARS-CoV-2 antibody titers in plasma from 24  
63 PCR-positive individuals and 10 PCR negative individuals by enzyme-linked immunosorbent  
64 assay (ELISA), pseudotyped virus neutralization assay, and authentic virus neutralization. Adult  
65 participants were enrolled in the prospective, adaptive cohort study of St. Jude Children's  
66 Research Hospital employees "St. Jude Tracking of Viral and Host Factors Associated with  
67 COVID-19" (SJTRC, [clinicaltrials.gov #NCT04362995](https://clinicaltrials.gov/ct2/show/study/NCT04362995)) beginning in April of 2020. SJTRC was  
68 approved by the St. Jude Internal Review Board, and all participants provided written informed  
69 consent in a manner consistent with institutional policies. Cohort characteristics are provided in  
70 Supplemental Table 1. Samples were collected from PCR-positive individuals a median 33 days  
71 following diagnosis (interquartile range: 25.75-48.25) between April and August 2020.

72 The ELISAs included in the comparison detect antibodies to SARS-CoV-2 spike protein,  
73 nucleocapsid protein (N), or the receptor-binding domain (RBD) of the spike protein as  
74 described<sup>15</sup>. Briefly, plasma samples were diluted 1:50 for RBD and N ELISAs and results  
75 expressed as the ratio of the optical density (OD) from the sample over the negative control (a  
76 known negative, pre-pandemic plasma sample), which is common practice. To determine spike  
77 titers, plasma was diluted 1:100 to 1:8100 and an area under the curve (AUC) analysis  
78 performed. The pseudotyped virus platform was a vesicular stomatitis virus (VSV) glycoprotein  
79 (G) knockout VSV expressing full-length SARS-CoV-2 spike protein (VSV-ΔG-S) from the  
80 Wuhan-Hu-1 strain with three different reporter genes: green fluorescence protein (GFP),  
81 luciferase (Luci.) and secreted alkaline phosphatase (SEAP). Authentic virus neutralization

82 studies were performed under BSL3+ conditions with the 2019n-CoV/USA\_WA1/2020 strain  
83 obtained from BEI Resources.

84 All PCR positive participants had ELISA titers to RBD, N, and spike, although the titers  
85 differed (Table 1). The average RBD ratio for the positive participants was 16.45 (95% CI: 14.53  
86 – 18.36) and 1.62 (95% CI: 1.33 – 1.91) for negative participants while the average N ratios  
87 were 9.20 (95% CI: 7.69 – 11.11) for positive participants and 1.40 (95% CI: 0.79 – 2.01) for  
88 negative participants. Spike AUC average was 6.44 (95% CI: 5.04 – 7.85) for the positive  
89 samples (the spike ELISA was not performed on negative samples).

90 To quantitate neutralization titers, plasma was diluted 1:100 to 1:900 and tested by  
91 authentic virus and VSV- $\Delta$ G-S GFP, Luci., and SEAP pseudotyped viruses. AUC and ND<sub>50</sub>  
92 were calculated (Table 2). The average AUC values for the authentic virus neutralization assay  
93 were 51.14 (95% CI: 43.01 – 62.25) for positive participants and 10.96 (95% CI: 6.29 – 15.63)  
94 for negative participants. The GFP, Luci, and SEAP pseudotyped virus neutralization assays  
95 gave average AUC values of 71.07 (95% CI: 65.47 – 76.67), 54.20 (95% CI: 46.67 – 61.73),  
96 and 56.14 (95% CI: 48.26 – 64.01) respectively, for positive participants and 9.33 (95% CI: 3.62  
97 – 15.04), 0 (95% CI: 0 – 0), and 1.21 (95% CI: 0 – 2.79) respectively for negative participants  
98 (Table 2). The geometric average ND<sub>50</sub> value for the authentic virus neutralization assay was  
99 254.7 (95% CI: 92.97 – 697.6) for positive participants and 13.56 (95% CI: 5.08 – 36.14) for  
100 negative participants compared to 1305 (95% CI: 763.5 – 2232), 404.1 (95% CI: 225.1 – 725.5),  
101 and 474.3 (95% CI: 255.7–879.7), for positive participants and 12.12 (95% CI: 3.562 – 41.27), 1  
102 (95% CI: 1 – 1), and 1.772 (95% CI: 0.7476 – 4.202) for negative participants respectively for  
103 the GFP, Luci and SEAP pseudotyped viruses. All neutralization platforms differentiated  
104 average negative and positive samples (Figure 1). While the AUC and ND<sub>50</sub> values were  
105 significantly higher for the GFP pseudotyped virus compared to the authentic virus or Luci.  
106 pseudotyped virus, suggesting that VSV- $\Delta$ G-S-GFP could be a more sensitive assay, it is  
107 balanced by increased AUC and ND<sub>50</sub> values in negative participants. Only the Luci. and SEAP

108 pseudotyped viruses showed no background in samples from PCR-negative participants. A  
109 Bland-Altman methods comparison test shows that there is systematic bias between the  
110 different pseudotyped virus neutralization assays and the authentic virus neutralization assay,  
111 leading to higher variability (highest for GFP pseudotypes) when the signal is low for each assay  
112 (Supplemental Figure 1). However, this bias decreases when signal becomes higher, resulting  
113 in the pseudotype assays becoming more concordant with authentic virus neutralization. The  
114 sigmoidal relationship between the amount of analyte detected and the readout in SEAP and  
115 luminescence assays could be a reason for the difference in bias between the pseudotyped  
116 virus assays. Variance at the lower end of the curve is less likely to be detected above  
117 background, compared to authentic virus neutralization and GFP pseudotyped virus  
118 neutralization where each infectious unit is counted, and variance has the same magnitude in  
119 both negative and positive samples. Furthermore, SEAP and luminescence detection kits often  
120 provide controls and stringent parameters for keeping background and noise to minimal levels.

121 To determine which neutralization platforms best correlated with authentic virus, linear  
122 regression analyses were performed. All pseudotyped virus neutralization platforms were  
123 significantly correlated to authentic virus neutralization regardless of the reporter with Luci.  
124 (Pearson's  $r = 0.765$ ) and SEAP (Pearson's  $r = 0.775$ ) having the highest correlations (Figure  
125 2A). The pseudotyped virus neutralization assays were significantly correlated with each other  
126 with Pearson's  $r$  values as high as 0.971 between the Luci. and SEAP assays. Linear  
127 regression analyses demonstrated that ELISA titers to the RBD (Pearson's  $r = 0.691$ ) and spike  
128 (Pearson's  $r = 0.648$ ) are also significantly correlated with authentic virus neutralization titers  
129 (Figure 2B). Nucleocapsid ELISA was significantly correlated with authentic virus neutralization,  
130 but has the worst correlation with authentic virus neutralization (Pearson's  $r = 0.514$ ), which has  
131 been shown previously for pseudotyped virus neutralization<sup>16</sup>. This is also congruent with the  
132 observation that antibodies targeting the RBD domain of spike are highly neutralizing<sup>17</sup>. A  
133 principle component analysis (PCA) was performed using all three ELISAs and all three

134 pseudotyped virus platforms as variables (Supplemental Figure 2). The resulting PCA plots  
135 shows distinct clustering of the samples with the highest authentic virus neutralization titers and  
136 a gradient from poorly neutralizing samples (in the bottom left) to highly neutralizing samples (in  
137 the top right). Finally, the average difference between the  $\log(\text{ND}_{50})$  for authentic virus  
138 neutralization and each pseudotyped virus neutralization is -0.487 for the GFP pseudotype,  
139 0.191 for the Luci. pseudotype, and 0.069 for the SEAP pseudotype.

140 To assess granularity in the different ELISA results, cut-off values were used to  
141 categorize responses as high positive, low positive, or negative. Determination of cut-off values  
142 (RBD ratio: 15, nucleocapsid ratio:10, and spike: 6) was done by finding internal nadir present in  
143 histograms for the different ELISAs. The stratification of RBD ELISA responses into high and  
144 low groups did not result in significantly different responses in any of the neutralization assays  
145 (Figure 3A), suggesting that high RBD values do not necessarily correlate to higher  
146 neutralization titers, despite RBD ELISA positivity being associated with neutralization (Figure  
147 2A). Similar results were obtained for the spike ELISA (Figure 3B) and nucleocapsid ELISA  
148 (Figure 3C). There was, however, a trend for increased neutralization in the high positive group  
149 versus the low positive group for each neutralization assay, regardless of ELISA assay,  
150 justifying future studies specifically designed to test the granularity of these assays. Congruent  
151 with the findings in Figure 2, highly positive ELISA results were significantly better at  
152 neutralizing than the negative samples for each ELISA.

153 While all the serological assays were significantly correlated with authentic virus  
154 neutralization, some assays performed better than others at predicting authentic virus  
155 neutralization (Supplemental Table 2). Based on correlation with authentic virus neutralization,  
156 the most accurate assays were the Luci. and SEAP pseudotyped virus neutralization assays.  
157 GFP pseudotyped virus neutralization, spike ELISA, and RBD ELISA form a second tier of  
158 assays which are still quite accurate at predicting authentic virus neutralization. Furthermore,  
159 the GFP pseudotyped virus neutralization was able to detect antibodies at significantly higher

160 dilutions than the other assays, making it the most sensitive assay tested. Despite nucleocapsid  
161 antigen being the basis for several common commercial antibody tests, nucleocapsid was the  
162 least predictive of authentic virus neutralization.

163 Collectively, these data demonstrate that VSV- $\Delta$ G pseudotyped virus neutralization  
164 platforms, especially Luci. and SEAP based platforms, are better at predicting authentic virus  
165 neutralization than ELISA regardless of the viral antigen tested. Not only are the Luci. and  
166 SEAP based pseudotype platforms most strongly correlated to authentic virus neutralization,  
167 they also have the lowest average difference in  $\log(\text{ND}_{50})$  compared to authentic virus  
168 neutralization. Previous reports have only compared ELISA titers to pseudotyped virus  
169 neutralization<sup>16</sup>, ELISA to authentic virus neutralization<sup>18</sup>, or only one type of ELISA and one  
170 pseudotyped virus platform against authentic virus neutralization<sup>10</sup>. Our studies provide one of  
171 the most comprehensive comparisons amongst multiple ELISA antigens, pseudotyped virus  
172 neutralization platforms, and authentic virus neutralization.

173 Of note, several spike and RBD positive samples showed very little authentic virus  
174 neutralization despite having moderate to high neutralization on the pseudotyped virus  
175 platforms. Furthermore, one sample appeared to show antibody dependent enhancement (ADE)  
176 in the authentic virus neutralization assay (1.8-fold increased plaque forming units (PFU)), but  
177 still showed low but detectable neutralization in all the pseudotyped virus platforms. While there  
178 is no definitive role for ADE during human SARS-CoV-2 infection, ADE has been demonstrated  
179 *in vitro* with other human coronaviruses<sup>19</sup>. Further characterization of this sample and screening  
180 for and characterizing similar samples will lead to a better understanding of the risk of ADE  
181 during SARS-CoV-2 infection. Recent evidence suggests that several SARS-CoV-2 variants,  
182 including B.1.351 and P.1, have decreased neutralization when treated with monoclonal  
183 antibodies or polyclonal sera derived from patients infected with early strains of SARS-CoV-2<sup>20-</sup>  
184 <sup>22</sup>. Future studies need to assess how the mutations present in the variants differentially affect  
185 ELISA, pseudotyped virus neutralization, and authentic virus neutralization.



186 In addition to accuracy, the serological assays differ in several key features  
187 (Supplemental Table 2), and the assay of choice may have to be determined by the settings.  
188 The requirement for a BSL3 laboratory makes authentic virus assays technically challenging  
189 and unfeasible for many clinical and research applications. This can be overcome by  
190 pseudotyped viruses. However, creation and validation of the different pseudotyped viruses is  
191 not trivial and read-outs may require specialized equipment (e.g. luminometer for the Luci.  
192 platform). Most laboratories have ready access to the equipment needed for performing ELISAs,  
193 making the technical requirements for these assays low. ELISAs can also be completed within  
194 several hours while the pseudotyped virus neutralization platforms require 12-24-hour  
195 incubations and authentic virus neutralization requires 48-72 hours. If all technical requirements  
196 have been met and are available, the assays are all relatively inexpensive, except for the Luci.  
197 platform which requires expensive reagents for reading the results. If turnaround time is a  
198 priority, the RBD and spike ELISAs would provide the fastest results with minor decreases in  
199 predicting authentic virus neutralization response. Alternatively, in resource-limited settings like  
200 field hospitals, the GFP based pseudotyped virus neutralization assay requires only a basic  
201 fluorescence microscope for readout and is more predictive of authentic virus neutralization than  
202 any of the ELISAs. Overall, this study shows that all six serological assays, to varying degrees,  
203 correlated with authentic virus neutralization, and the optimal serological assay for assessing a  
204 protective antibody response is going to be institution and question specific.

205

206 Table 1: SARS-CoV-2 Protein ELISA Values

| PCR      | Sample | ELISA                          |                              |                      |
|----------|--------|--------------------------------|------------------------------|----------------------|
|          |        | RBD ratio<br>(sample/negative) | N ratio<br>(sample/negative) | Spike<br>(AUC x 100) |
| Positive | 1      | 17.92                          | 13.75                        | 9.26                 |
| Positive | 2      | 16.48                          | 14.00                        | 12.90                |
| Positive | 3      | 9.62                           | 7.20                         | 3.36                 |
| Positive | 4      | 8.79                           | 4.45                         | 1.97                 |
| Positive | 5      | 18.41                          | 8.74                         | 14.19                |
| Positive | 6      | 10.56                          | 6.46                         | 8.21                 |
| Positive | 7      | 12.01                          | 6.20                         | 3.43                 |
| Positive | 8      | 19.10                          | 16.61                        | 11.38                |
| Positive | 9      | 15.54                          | 5.85                         | 2.87                 |
| Positive | 10     | 16.73                          | 10.95                        | 3.08                 |
| Positive | 11     | 21.74                          | 9.42                         | 5.30                 |
| Positive | 12     | 24.08                          | 14.14                        | 7.24                 |
| Positive | 13     | 20.13                          | 15.73                        | 3.97                 |
| Positive | 14     | 19.59                          | 13.09                        | 5.39                 |
| Positive | 15     | 8.12                           | 5.32                         | 2.43                 |
| Positive | 16     | 13.76                          | 10.37                        | 3.89                 |
| Positive | 17     | 6.94                           | 5.59                         | 3.51                 |
| Positive | 18     | 21.43                          | 5.11                         | 12.55                |
| Positive | 19     | 21.20                          | 1.76                         | 5.04                 |
| Positive | 20     | 18.76                          | 8.33                         | 8.03                 |
| Positive | 21     | 20.48                          | 17.47                        | 6.39                 |
| Positive | 22     | 18.39                          | 9.25                         | 7.29                 |
| Positive | 23     | 17.04                          | 9.90                         | 6.26                 |
| Positive | 24     | 17.90                          | 5.82                         | 6.74                 |
| Negative | 25     | 1.04                           | 0.71                         |                      |
| Negative | 26     | 2.15                           | 1.14                         |                      |
| Negative | 27     | 1.80                           | 1.17                         |                      |
| Negative | 28     | 1.72                           | 2.81                         |                      |
| Negative | 29     | 2.27                           | 3.57                         |                      |
| Negative | 30     | 0.99                           | 0.94                         |                      |
| Negative | 31     | 1.99                           | 1.01                         |                      |
| Negative | 32     | 1.45                           | 0.68                         |                      |
| Negative | 33     | 1.75                           | 1.25                         |                      |
| Negative | 34     | 1.07                           | 0.75                         |                      |

207

208

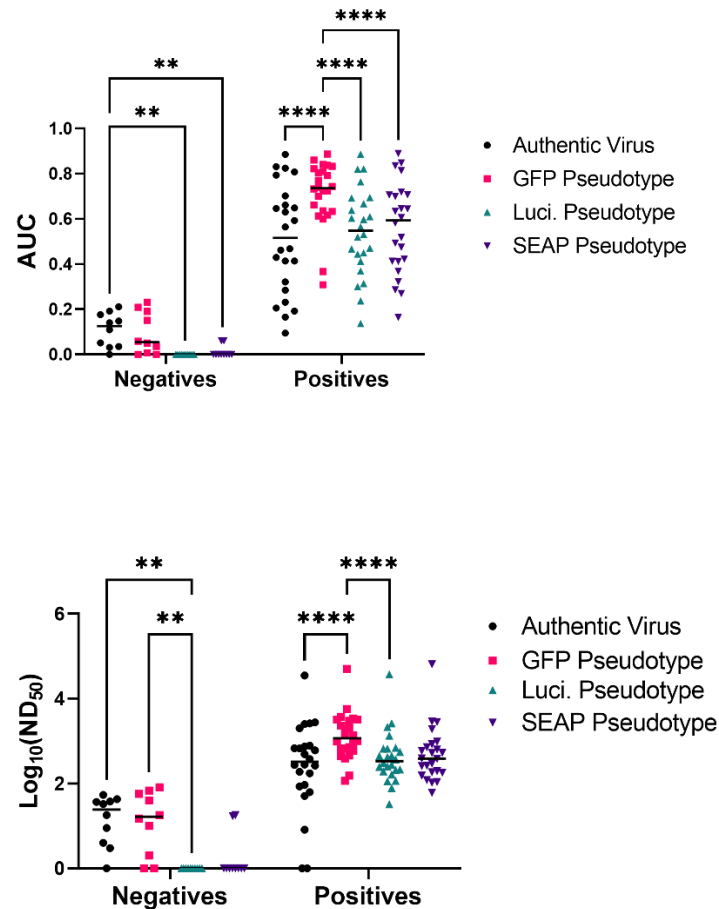
209 Table 2: Authentic Virus and Pseudotyped Virus Neutralization Summary Statistics

| PCR      | Sample | Authentic Virus |                  | GFP Pseudotype |                  | Luci. Pseudotype |                  | SEAP Pseudotype |                  |
|----------|--------|-----------------|------------------|----------------|------------------|------------------|------------------|-----------------|------------------|
|          |        | AUC             | ND <sub>50</sub> | AUC            | ND <sub>50</sub> | AUC              | ND <sub>50</sub> | AUC             | ND <sub>50</sub> |
| Positive | 1      | 0.565           | 380              | 0.739          | 908              | 0.520            | 276              | 0.582           | 382              |
| Positive | 2      | 0.630           | 671              | 0.804          | 2305             | 0.692            | 662              | 0.645           | 535              |
| Positive | 3      | 0.166           | 1                | 0.367          | 153              | 0.137            | 33               | 0.164           | 60               |
| Positive | 4      | 0.321           | 1                | 0.309          | 116              | 0.237            | 78               | 0.287           | 109              |
| Positive | 5      | 0.831           | 2527             | 0.860          | 5744             | 0.821            | 2162             | 0.836           | 2834             |
| Positive | 6      | 0.662           | 745              | 0.723          | 1505             | 0.668            | 692              | 0.706           | 722              |
| Positive | 7      | 0.206           | 51               | 0.661          | 672              | 0.467            | 253              | 0.412           | 181              |
| Positive | 8      | 0.794           | 2612             | 0.810          | 2997             | 0.764            | 1341             | 0.814           | 1922             |
| Positive | 9      | 0.095           | 8                | 0.613          | 665              | 0.314            | 112              | 0.322           | 121              |
| Positive | 10     | 0.284           | 86               | 0.633          | 586              | 0.412            | 193              | 0.368           | 154              |
| Positive | 11     | 0.649           | 782              | 0.822          | 3747             | 0.531            | 307              | 0.518           | 296              |
| Positive | 12     | 0.702           | 682              | 0.792          | 1995             | 0.597            | 447              | 0.645           | 527              |
| Positive | 13     | 0.646           | 606              | 0.837          | 3229             | 0.638            | 551              | 0.606           | 392              |
| Positive | 14     | 0.468           | 275              | 0.701          | 716              | 0.444            | 208              | 0.413           | 186              |
| Positive | 15     | 0.232           | 93               | 0.599          | 462              | 0.301            | 116              | 0.269           | 105              |
| Positive | 16     | 0.825           | 2769             | 0.833          | 2317             | 0.820            | 2606             | 0.848           | 2910             |
| Positive | 17     | 0.429           | 281              | 0.770          | 3222             | 0.470            | 248              | 0.493           | 259              |
| Positive | 18     | 0.886           | 35373            | 0.887          | 50378            | 0.886            | 37272            | 0.890           | 64851            |
| Positive | 19     | 0.808           | 2008             | 0.842          | 3409             | 0.694            | 662              | 0.700           | 635              |
| Positive | 20     | 0.593           | 495              | 0.733          | 983              | 0.565            | 369              | 0.634           | 589              |
| Positive | 21     | 0.414           | 175              | 0.744          | 1373             | 0.603            | 417              | 0.707           | 850              |
| Positive | 22     | 0.462           | 266              | 0.724          | 1001             | 0.610            | 444              | 0.719           | 972              |
| Positive | 23     | 0.192           | 63               | 0.636          | 390              | 0.450            | 215              | 0.423           | 197              |
| Positive | 24     | 0.414           | 190              | 0.617          | 441              | 0.370            | 163              | 0.474           | 266              |
| Negative | 25     | 0.031           | 9                | 0.151          | 40               | 0.000            | 1                | 0.000           | 1                |
| Negative | 26     | 0.035           | 3                | 0.191          | 57               | 0.000            | 1                | 0.000           | 1                |
| Negative | 27     | 0.141           | 33               | 0.035          | 10               | 0.000            | 1                | 0.000           | 1                |
| Negative | 28     | 0.212           | 54               | 0.007          | 2                | 0.000            | 1                | 0.000           | 1                |
| Negative | 29     | 0.176           | 43               | 0.051          | 15               | 0.000            | 1                | 0.060           | 18               |
| Negative | 30     | 0.000           | 1                | 0.231          | 82               | 0.000            | 1                | 0.000           | 1                |
| Negative | 31     | 0.192           | 37               | 0.000          | 1                | 0.000            | 1                | 0.060           | 17               |
| Negative | 32     | 0.110           | 18               | 0.209          | 68               | 0.000            | 1                | 0.000           | 1                |
| Negative | 33     | 0.051           | 4                | 0.000          | 1                | 0.000            | 1                | 0.000           | 1                |
| Negative | 34     | 0.148           | 38               | 0.059          | 18               | 0.000            | 1                | 0.000           | 1                |

210

211

212 Figure 1



213

214

215 **Figure 1: Comparison of neutralization assays by sample groups.** Area under the curve

216 (AUC) (top) and neutralization dilution – 50% (ND<sub>50</sub>) (bottom) calculations by neutralization

217 assay type. AUC and ND<sub>50</sub> values were calculated and used to compare authentic virus

218 neutralization (black), GFP pseudotype neutralization (pink), luciferase pseudotype (teal), and

219 SEAP pseudotype (purple). \* p < 0.05, \*\* p < 0.01, \*\*\*p < 0.001 (mixed-effects model with the

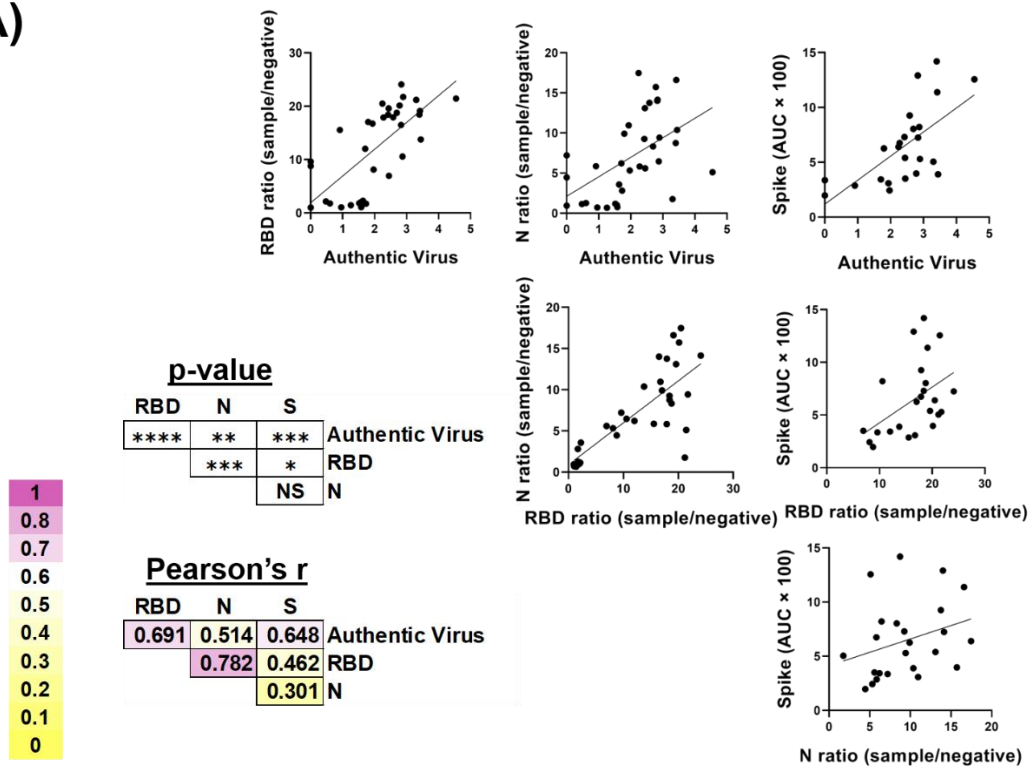
220 Geisser-Greenhouse correction and Tukey multiple comparisons post-test and p-value

221 adjustment). n = 34 samples run on each assay.

222

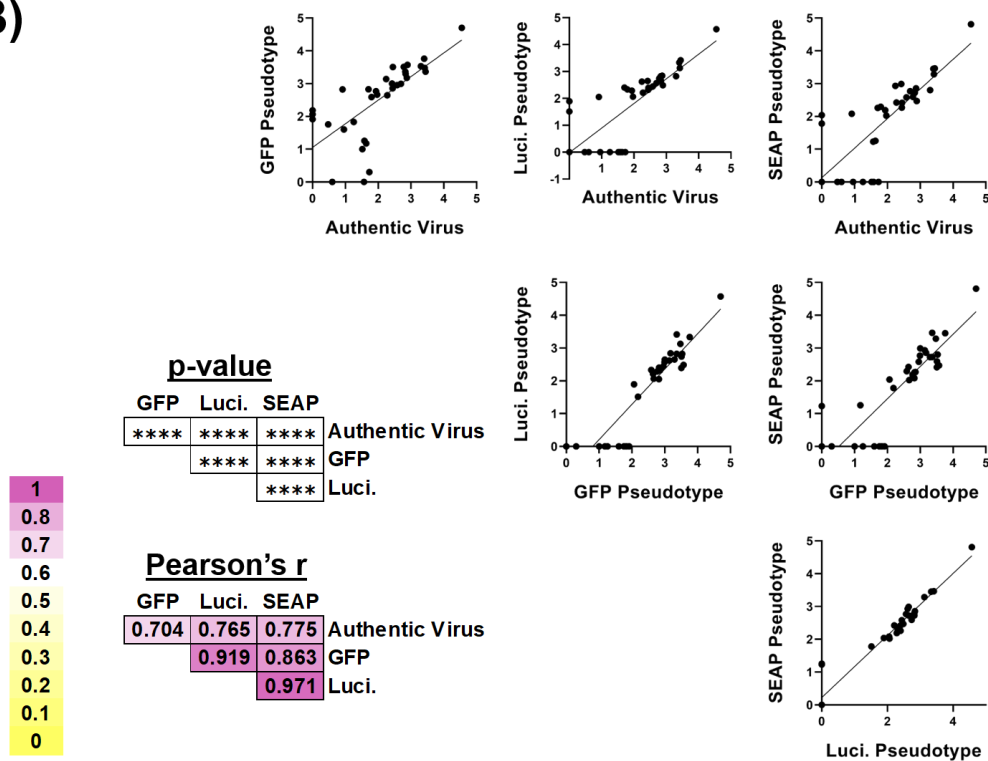
223 Figure 2

A)



224

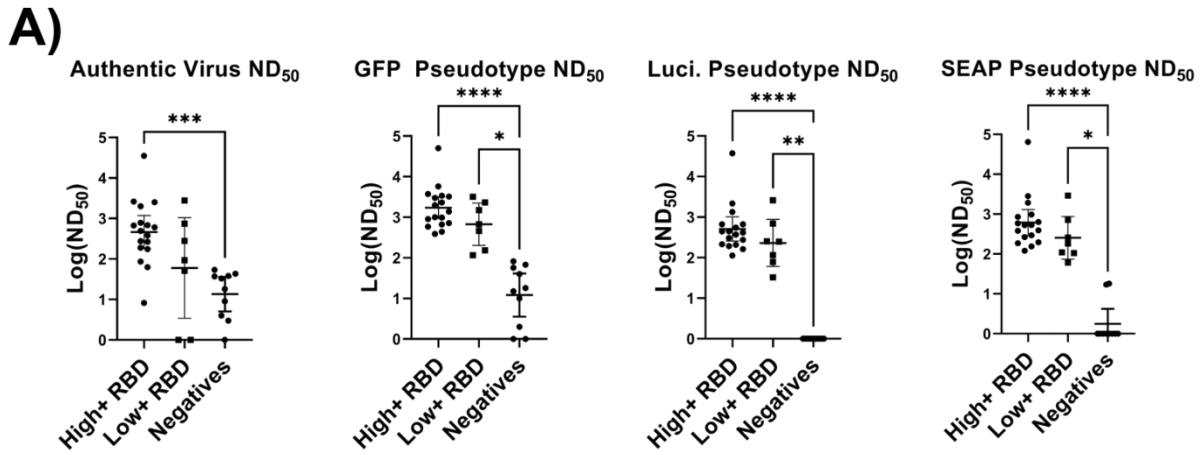
B)



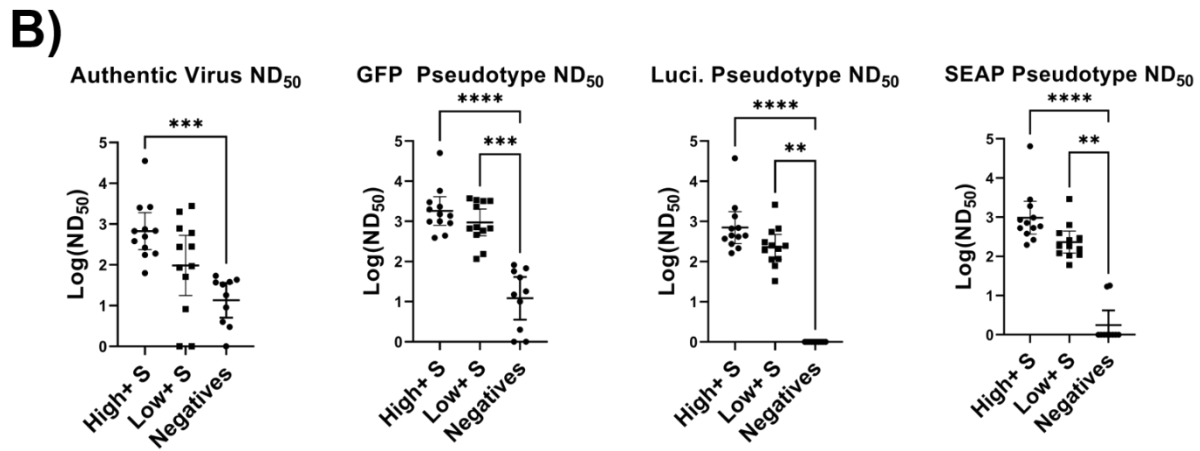
225

226 **Figure 2: Correlation of SARS-CoV-2 serologic assays.** A) SARS-CoV-2 specific ELISA  
227 assays and B) VSV pseudotyped virus neutralization assays were compared by simple linear  
228 regression. The Pearson's r values (a metric of correlation) and p-values corresponding to each  
229 graph are to the lower left of each set of graphs. The shade of background corresponds to the  
230 degree of correlation between the two assays. \*  $p < 0.05$ , \*\*  $p < 0.01$ , \*\*\*  $p < 0.001$ , \*\*\*\*  $p <$   
231  $0.0001$ .  
232

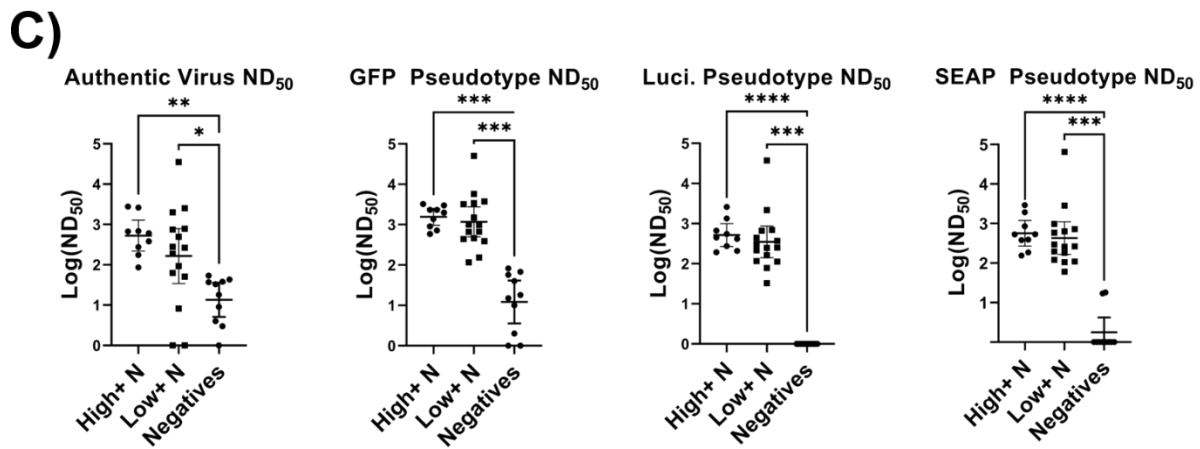
233 Figure 3



234



235



236

237

238 **Figure 3: Comparison of high positive, low positive, and negative ELISA groups across**  
239 **neutralization assays.** A) RBD B) spike (S) and C) nucleocapsid (N) positive samples were  
240 divided into high and low positives by finding cut off values using histograms (RBD ratio: 15, N  
241 ratio: 10, and Spike: 6). Log( $ND_{50}$ ) values for the corresponding samples were then graphed  
242 and compared by Kruskal-Wallis test with Dunn's multiple comparisons tests. Significance  
243 thresholds: \*  $p < 0.05$ , \*\*  $p < 0.01$ , \*\*\*  $p < 0.001$ , p \*\*\*\*  $p < 0.0001$ .  
244



245 **References**

246

- 247 1 Corman, V. M. *et al.* Detection of 2019 novel coronavirus (2019-nCoV) by real-time RT-  
248 PCR. *Euro Surveill* **25**, 2000045, doi:10.2807/1560-7917.ES.2020.25.3.2000045 (2020).
- 249 2 Wang, W., Tang, J. & Wei, F. Updated understanding of the outbreak of 2019 novel  
250 coronavirus (2019-nCoV) in Wuhan, China. *Journal of medical virology* **92**, 441-447,  
251 doi:10.1002/jmv.25689 (2020).
- 252 3 Wu, F. *et al.* A new coronavirus associated with human respiratory disease in China.  
253 *Nature* **579**, 265-269, doi:10.1038/s41586-020-2008-3 (2020).
- 254 4 Zhou, P. *et al.* A pneumonia outbreak associated with a new coronavirus of probable bat  
255 origin. *Nature* **579**, 270-273, doi:10.1038/s41586-020-2012-7 (2020).
- 256 5 Grzelak, L. *et al.* A comparison of four serological assays for detecting anti-SARS-CoV-  
257 2 antibodies in human serum samples from different populations. *Science translational*  
258 *medicine* **12**, eabc3103, doi:10.1126/scitranslmed.abc3103 (2020).
- 259 6 Pérez-García, F. *et al.* Comparative evaluation of six immunoassays for the detection of  
260 antibodies against SARS-CoV-2. *Journal of virological methods*, 114047,  
261 doi:10.1016/j.jviromet.2020.114047 (2020).
- 262 7 Whitman, J. D. *et al.* Evaluation of SARS-CoV-2 serology assays reveals a range of test  
263 performance. *Nature Biotechnology* **38**, 1174-1183, doi:10.1038/s41587-020-0659-0  
264 (2020).
- 265 8 Ju, B. *et al.* Human neutralizing antibodies elicited by SARS-CoV-2 infection. *Nature*  
266 **584**, 115-119, doi:10.1038/s41586-020-2380-z (2020).
- 267 9 van der Heide, V. Neutralizing antibody response in mild COVID-19. *Nature Reviews*  
268 *Immunology* **20**, 352-352, doi:10.1038/s41577-020-0325-2 (2020).

- 269 10 von Rhein, C. *et al.* Comparison of potency assays to assess SARS-CoV-2 neutralizing  
270 antibody capacity in COVID-19 convalescent plasma. *Journal of virological methods*  
271 **288**, 114031-114031, doi:10.1016/j.jviromet.2020.114031 (2020).
- 272 11 Yu, J. *et al.* DNA vaccine protection against SARS-CoV-2 in rhesus macaques. *Science*  
273 **369**, 806, doi:10.1126/science.abc6284 (2020).
- 274 12 Polack, F. P. *et al.* Safety and Efficacy of the BNT162b2 mRNA Covid-19 Vaccine. *New*  
275 *England Journal of Medicine*, doi:10.1056/NEJMoa2034577 (2020).
- 276 13 Deshpande, G. *et al.* Neutralizing antibody responses to SARS-CoV-2 in COVID-19  
277 patients. *Indian Journal of Medical Research* **152**, 82-87,  
278 doi:10.4103/ijmr.IJMR\_2382\_20 (2020).
- 279 14 Oguntuyo, K. Y. *et al.* Quantifying absolute neutralization titers against SARS-CoV-2 by  
280 a standardized virus neutralization assay allows for cross-cohort comparisons of COVID-  
281 19 sera. *medRxiv*, doi:10.1101/2020.08.13.20157222 (2020).
- 282 15 Amanat, F. *et al.* A serological assay to detect SARS-CoV-2 seroconversion in humans.  
283 *Nature Medicine* **26**, 1033-1036, doi:10.1038/s41591-020-0913-5 (2020).
- 284 16 McAndrews, K. M. *et al.* Heterogeneous antibodies against SARS-CoV-2 spike receptor  
285 binding domain and nucleocapsid with implications for COVID-19 immunity. *JCI Insight*  
286 **5**, doi:10.1172/jci.insight.142386 (2020).
- 287 17 Piccoli, L. *et al.* Mapping Neutralizing and Immunodominant Sites on the SARS-CoV-2  
288 Spike Receptor-Binding Domain by Structure-Guided High-Resolution Serology. *Cell*  
289 **183**, 1024-1042.e1021, doi:10.1016/j.cell.2020.09.037 (2020).
- 290 18 Heaney, C. D. *et al.* Comparative performance of multiplex salivary and commercially  
291 available serologic assays to detect SARS-CoV-2 IgG and neutralization titers. *medRxiv*,  
292 doi:10.1101/2021.01.28.21250717 (2021).

- 293 19 Lee, W. S., Wheatley, A. K., Kent, S. J. & DeKosky, B. J. Antibody-dependent  
294 enhancement and SARS-CoV-2 vaccines and therapies. *Nature Microbiology* **5**, 1185-  
295 1191, doi:10.1038/s41564-020-00789-5 (2020).
- 296 20 Chen, R. E. *et al.* Resistance of SARS-CoV-2 variants to neutralization by monoclonal  
297 and serum-derived polyclonal antibodies. *Nature Medicine*, doi:10.1038/s41591-021-  
298 01294-w (2021).
- 299 21 Hoffmann, M. *et al.* SARS-CoV-2 variants B.1.351 and B.1.1.248: Escape from  
300 therapeutic antibodies and antibodies induced by infection and vaccination. *bioRxiv*,  
301 2021.2002.2011.430787, doi:10.1101/2021.02.11.430787 (2021).
- 302 22 Wang, P. *et al.* Antibody Resistance of SARS-CoV-2 Variants B.1.351 and B.1.1.7.  
303 *Nature*, doi:10.1038/s41586-021-03398-2 (2021).
- 304
- 305

306 **Methods**

307

308 **Data Availability**

309 Authors can confirm that all relevant data are included in the paper and/or its supplementary  
310 information files.

311

312 **RBD/N ELISA**

313 SARS-CoV-2 RBD protein was diluted to a concentration of 1.5 µg/ml in PBS and added at 50  
314 µl per well to a 96-well ELISA plate. The ELISA plates were sealed and allowed to incubate at  
315 4°C overnight. The next day the coating solution was removed, and the plates were blocked at  
316 room temperature (RT) using 3% milk (200 µl per well) for a minimum of 1 hour but not  
317 exceeding 4 hours. While the plates were being blocked, the samples were prepared by diluting  
318 the plasma 1:50 in 1% milk. Following the blocking period, the milk was removed, and the plates  
319 were washed 3x with 0.1% phosphate buffered saline containing 0.1% Tween-20 (PBS-T) using  
320 200 µl per well. The diluted plasma was added to the blocked plate at 50 µl per well along with 2  
321 positive controls (α SARS-CoV-2 RBD antibody at 1:5000, 1:25000, 1:125000, and 1:625000  
322 dilutions and plasma from a naturally infected donor at a 1:50 dilution) and a known negative,  
323 pre-pandemic plasma sample (1:50). The samples were incubated for 1.5 hours at RT and then  
324 removed and washed 3x with 200 µl 0.1% PBS-T. Goat α human IgG horseradish peroxidase  
325 (HRP) conjugated secondary antibody was diluted 1:2500 in 1% milk and 50 µl was added to  
326 each well of the washed plate and incubated at RT for 30 minutes. Following the incubation  
327 period, the secondary was removed, and the plate was washed 3x with 0.1% PBS-T. OPD  
328 substrate was prepared directly before use and added at 50 µl per well for exactly 8 minutes.  
329 The O-phenylenediamine dihydrochloride (OPD) substrate was stopped by adding 50 µl of 3M  
330 HCl and then the plate was read using a spectrophotometer at 490nm.

331

332 **Spike ELISA**

333 SARS-CoV-2 spike protein was diluted to a concentration of 2 µg/ml in PBS and added at 50 µl  
334 per well to a 96-well ELISA plate. The ELISA plates were sealed and allowed to incubate at 4°C  
335 overnight. The next day the coating solution was removed, and the plates were blocked using  
336 3% milk (200 µl per well) for a minimum of 1 hour but not exceeding 4 hours. While the plates  
337 were being blocked, the samples were prepared by creating a 3-fold serial dilution starting at  
338 1:100 and ending at 1:8100 (1% milk as diluent). Following the blocking period, the milk was  
339 removed, and the plates were washed 3x with 0.1% PBS-T using 200 µl per well. The diluted  
340 plasma was added to the blocked plate at 50 µl per well along with 2 positive controls (α SARS-  
341 CoV-2 RBD antibody at 1:5000, 1:25000, 1:125000, and 1:625000 dilutions and plasma from a  
342 naturally infected donor at 1:100, 1:300, 1:900, 1:2700, and 1:8100 dilutions) and a known  
343 negative, pre-pandemic plasma sample (1:100). The samples were incubated for 1.5 hours at  
344 RT and then removed and washed 3x with 200 µl 0.1% PBS-T. Goat α human IgG HRP  
345 conjugated secondary antibody was diluted 1:2500 in 1% milk and 50 µl was added to each well  
346 of the washed plate and incubated at RT for 30 minutes. Following the incubation period, the  
347 secondary was removed, and the plate was washed 3x with 0.1% PBS-T. OPD substrate was  
348 prepared directly before use and added at 50 µl per well for exactly 8 minutes. The OPD  
349 substrate was stopped by adding 50 µl of HCL acid and then the plate was read using a  
350 spectrophotometer at 490nm. Spike data is presented as either AUC or AUC × 100 in order to  
351 plot it on the same scale as the other ELISAs.

352

353 **Tissue culture**

354 VeroE6 cells stably expressing TMPRSS2 (Vero-TMPRSS2) (XenoTech) were cultured in  
355 Eagle's Minimal Essential Medium (EMEM) supplemented with 10% fetal bovine serum (FBS),  
356 100 U/mL penicillin, 100 µg/mL streptomycin, and 2 mM GlutaMax (Gibco). Media was

357 supplemented with 1 mg/mL G418 every other passage. All tissue culture was performed in a  
358 humidified incubator set to 37° C and 5% CO<sub>2</sub>.

359

### 360 **SARS-CoV-2 neutralizing antibody assay**

361 Serially diluted plasma samples were mixed with diluted (approximately 6 PFU/cm<sup>2</sup>) SARS-  
362 CoV-2 (2019n-CoV/USA\_WA1/2020) in EMEM supplemented with 5% FBS, 100 U/mL  
363 penicillin, 100 µg/mL streptomycin, and 2 mM GlutaMax. Mixtures were incubated for 1 h in a  
364 humidified incubator at 37° C and 5% CO<sub>2</sub>. After 1 h, culture media was removed from  
365 approximately 90% confluent Vero-TMPRSS2 cells grown in 6-well plates and replaced with  
366 virus/plasma mixtures. Plates were returned to the incubator for 1 h at 37° C and 5% CO<sub>2</sub>.  
367 Plates were rocked manually every 15 minutes. After incubation, an agarose overlay containing  
368 Minimal Essential Media (MEM) supplemented with 5% FBS 100 U/mL penicillin, 100 µg/mL  
369 streptomycin, 2 mM GlutaMax, 0.075% sodium bicarbonate, 0.01 M 4-(2-hydroxyethyl)-1-  
370 piperazineethanesulfonic acid (HEPES), and 1% low melting temperature agarose (SeaPlaque;  
371 Lonza) was added to each well. Once agarose hardened at  
372 RT, plates were returned to the incubator at 37° C and 5% CO<sub>2</sub>. After 48 h, cells were fixed with  
373 10% neutral buffered formalin for 1 h, the agar plugs were removed, and then cells were stained  
374 with crystal violet for 5 – 10 minutes. Upon rinsing with H<sub>2</sub>O, plaques were visualized and  
375 counted. All samples were run in duplicate

376

### 377 **VSV-ΔG-GFP-SARS-CoV-2-S Neutralizing antibody assay**

378 Serially diluted plasma samples were mixed with diluted and mixed with Spike/VSV-ΔG-GFP  
379 pseudotypes in EMEM supplemented with 5% FBS, 100 U/mL penicillin, 100 µg/mL  
380 streptomycin, and 2 mM GlutaMax. Mixtures were incubated for 1 h in a humidified incubator at  
381 37° C and 5% CO<sub>2</sub>. After 1 h, culture media was removed from approximately 90% confluent  
382 Vero-TMPRSS2 cells grown in 96-well plates and replaced with virus/plasma mixtures. Plates

383 were returned to the incubator at 37° C and 5% CO<sub>2</sub>. After 24 h, IU were quantified manually  
384 using an EVOS fluorescence microscope. All samples run in duplicate.

385

### 386 **Luciferase Assay**

387 20 hours prior to assay set up, Vero-TMRSS2 were plated in a 96-well plate at 20,000 cells per  
388 well in DMEM supplemented with 5% FBS and 1 mg/mL G418. For assay set up, plasma  
389 samples were initially diluted 1:100 and serially diluted 1:3 in DMEM supplemented with 5%  
390 FBS. Diluted samples were mixed 1:1 with Spike/VSV-ΔG-Luciferase pseudotyped virus diluted  
391 to final 250 IU per well in serum free DMEM. Mixtures were incubated for 1 hour in a humidified  
392 incubator at 37° C and 5% CO<sub>2</sub>. After the incubation period, culture medium was removed from  
393 Vero-TMPRSS2 cells and virus/plasma mixture was added to the cells in triplicate. Plates were  
394 incubated for approximately 18 hours in a humidified incubator at 37° C and 5% CO<sub>2</sub>. After the  
395 incubation period, Luc-Screen Extended-Glow (ThermoFisher) buffers were added to the wells  
396 according to manufacturer's instructions and incubated for a minimum of 10 minutes at room  
397 temperature protected from light. Luminescence was measured with a luminometer using one  
398 second integration time.

399

### 400 **SEAP Assay**

401 20 hours prior to assay set up, Vero-TMRSS2 were plated in a 96-well plate at 20,000 cells per  
402 well in DMEM supplemented with 5% FBS and 1 mg/mL G418. For assay set up, plasma  
403 samples were initially diluted 1:100 and serially diluted 1:3 in DMEM supplemented with 5%  
404 FBS. Diluted samples were mixed 1:1 with purified Spike/VSV-ΔG--SEAP pseudotyped virus  
405 diluted to final 250 IU per well in serum free DMEM. Mixtures were incubated for 1 hour in a  
406 humidified incubator at 37° C and 5% CO<sub>2</sub>. After the incubation period, culture medium was  
407 removed from Vero-TMPRSS2 cells and virus/plasma mixture was added to the cells in  
408 triplicate. Plates were incubated for approximately 28 hours in a humidified incubator at 37° C

409 and 5% CO<sub>2</sub>. After the incubation period, Quanti-Blue (InvivoGen) solution was combined with  
410 20 µL supernatant according to manufacturer's instructions and incubated for a minimum of 15  
411 minutes at 37° C protected from light. Optical density was measured at 620-655 nm.

412

### 413 **SARS-CoV-2/VSV pseudotype production**

414 VSV-ΔG pseudotypes displaying the full-length SARS-CoV-2 spike (Wuhan-Hu-1 strain) were  
415 generated essentially as described<sup>23</sup> with the following modifications. Baby hamster kidney  
416 (BHK-21) cells in 10 cm dishes were transfected using Lipofectamine 2000 according to the  
417 manufacturer's instructions with 24 µg of a plasmid encoding a codon-optimized cDNA for the  
418 SARS-CoV-2 spike<sup>15</sup>, which was generously provided by Florian Krammer. Approximately 20-24  
419 hours later the transfected cells were infected at a multiplicity of 5 with VSV-G pseudotyped ΔG-  
420 GFP, luciferase, or SEAP. Virus was adsorbed for 1 hr, the inoculum was removed, cells were  
421 rinsed once with serum-free DMEM and then 4 ml of hybridoma supernatant containing the I1  
422 monoclonal antibody<sup>24</sup> was added for 30 minutes to neutralize residual VSV-ΔG pseudotyped  
423 virus from the inoculum and then replaced with DMEM containing 20% fetal bovine serum. The  
424 supernatant containing the spike-ΔG pseudotypes was collected 22-24 hours later, cell debris  
425 was removed by centrifugation at 450 x g for 10 minutes. For the ΔG-GFP and luciferase  
426 pseudotypes, the supernatant was aliquoted and stored at -80° C. For the ΔG-SEAP  
427 pseudotypes, the supernatant was transferred to a Beckman SW41 tube, underlayered with  
428 sterile 20% sucrose in PBS, and virus was pelleted at 35,000 rpm for 45 minutes in a SW41  
429 swinging bucket rotor. Pelleting virus was required to separate it from SEAP released from the  
430 infected cells. The pellets were resuspended in DMEM containing 20% FBS and stored at -80°  
431 C.

432

### 433 **Statistics**



434 Area under the curve (AUC) and neutralization dilution – 50% (ND<sub>50</sub>) analyses were performed  
435 in GraphPad Prism (version 9.0.0): non-linear regression (dose-response). Pearson's r values  
436 for comparing assays by percent maximum AUC were calculating using simple linear regression  
437 analysis in GraphPad Prism. AUC and ND<sub>50</sub> values for the different assays were compared by  
438 mixed-effects model with the Geisser-Greenhouse correction and Tukey multiple comparisons  
439 post-test and p-value adjustment in GraphPad Prism (version 9.0.0). Kruskal-Wallis tests with  
440 Dunn's multiple comparisons tests. were performed to compare neutralizing antibody responses  
441 between highly positive ELISA samples, low positive ELISA samples, and negative samples.  
442 Principle component analysis (PCA) was performed in GraphPad Prism (version 9.0.0) with  
443 principle components selected based on parallel analysis. A 95% percentile level was used, and  
444 1000 simulations were performed for the PCA. The Bland-Altman analyses were performed in  
445 GraphPad Prism (version 9.0.0).  
446

447 Methods References

- 448 15 Amanat, F. *et al.* A serological assay to detect SARS-CoV-2 seroconversion in humans.  
449 *Nature Medicine* **26**, 1033-1036, doi:10.1038/s41591-020-0913-5 (2020).
- 450 23 Whitt, M. A. Generation of VSV pseudotypes using recombinant  $\Delta$ G-VSV for studies on  
451 virus entry, identification of entry inhibitors, and immune responses to vaccines. *Journal*  
452 *of virological methods* **169**, 365-374, doi:10.1016/j.jviromet.2010.08.006 (2010).
- 453 24 Lefrancois, L. & Lyles, D. S. The interaction of antibody with the major surface  
454 glycoprotein of vesicular stomatitis virus. I. Analysis of neutralizing epitopes with  
455 monoclonal antibodies. *Virology* **121**, 157-167 (1982).
- 456
- 457

458 **Acknowledgements**

459 The authors wish to thank Amy E. Davis, Virginia Hargest, Rebekah Honce, Brandi Livingston,  
460 Victoria Meliopoulos, Bridgett Sharp, Maria Smith, and Kristin Wiggins for aiding the Schultz-  
461 Cherry lab's COVID-19 response; the members of the Thomas, McGargill, and Schultz-Cherry  
462 labs for technical assistance and feedback on the work; Dr. Gang Wu and the Center for  
463 Applied Bioinformatics at St. Jude along with Michael Meagher, Timothy Lockey, and the St.  
464 Jude Good Manufacturing Practice (GMP) facility; Tamanna Shamrin and Rishi Kodela for  
465 creation and management of the clinical database. This work was funded by ALSAC, the NIAID  
466 for the St. Jude Center of Excellence for Influenza Research and Surveillance (CEIRS contract  
467 HHSN27220140006C) and the NIAID Collaborative Influenza Vaccine Innovation Centers  
468 (CIVIC) contract 75N93019C00052, and by the University of Tennessee Research Foundation.  
469 JHE is supported by the American Society of Hematology Scholar Award. Work in the Krammer  
470 laboratory is partially funded by the NIAID Collaborative Influenza Vaccine Innovation Centers  
471 (CIVIC) contract 75N93019C00051, NIAID Center of Excellence for Influenza Research and  
472 Surveillance (CEIRS, contract # HHSN272201400008C), by the generous support of the Cohen  
473 Foundation, the JPB Foundation and the Open Philanthropy Project (research grant 2020-  
474 215611 (5384), and by anonymous donors.

475

476 **Author contributions**

477 Conceptualization: N.W., K.W., S.C., E.K.R., S.S.-C.  
478 Conception, design, and oversight of parent study; SJTRC: J.H., H.H., K.J.A., R.D., A.H.G.,  
479 J.H.E., J.W., and P.G.T.  
480 Formal Analysis: NW., K.W., S.C., E.K.R., T.M., L.T.  
481 Investigation: N.W., K.W., S.C., E.K.R.  
482 Methodology: NW., K.W., S.C., E.K.R., C.Y.L. E.K.A., P.F., M.A.M.  
483 Resources: F.K., M.A.W.

484 Sample acquisition and curation: K.J.A., A.G., A.H.G., E.K.A., J.H.E., J.W., and P.G.T.

485 Writing, original draft: N.W., E.K.R.

486 Writing, review, and editing: N.W., K.W., S.C., E.K.R., M.A.W., H.H., J.H.E., A.H.G., T.M., T.L.,

487 D.R.H., M.A.M., F.K., J.W., P.G.T., S.S.-C.

488 Visualization: N.W.

489 Supervision: S.S.-C.

490

491 **Competing interest's declaration**

492 The Icahn School of Medicine at Mount Sinai has filed patent applications relating to SARS-

493 CoV-2 serological assays and NDV-based SARS-CoV-2 vaccines which name FK as inventor.

494 FK would also like to note the following, which could be perceived as a conflict of interest: He

495 has previously published work on influenza virus vaccines with S. Gilbert (University of Oxford),

496 has consulted for Curevac, Merck and Pfizer (before 2020), is currently consulting for Pfizer,

497 Seqirus and Avimex, his laboratory is collaborating with Pfizer on animal models of SARS-CoV-

498 2, his laboratory is collaborating with N. Pardi at the University of Pennsylvania on mRNA

499 vaccines against SARS-CoV-2, his laboratory was working in the past with GlaxoSmithKline on

500 the development of influenza virus vaccines and two of his mentees have recently joined

501 Moderna. No other others have conflicts of interest to report.